Holzforschung, Vol. 62, pp. 230–236, 2008 • Copyright © by Walter de Gruyter • Berlin • New York. DOI 10.1515/HF.2008.050

Effect of thermo-mechanical refining pressure on the properties of wood fibers as measured by nanoindentation and atomic force microscopy

Cheng Xing[1], Siqun Wang[1,*], George M. Pharr[2,3] and Leslie H. Groom[4]

[1] Tennessee Forest Products Center, The University of Tennessee, Knoxville, TN, USA
[2] Department of Material Science, The University of Tennessee, Knoxville, TN, USA
[3] Metals and Ceramic Division, Oak Ridge National Laboratory, Oak Ridge, TN, USA
[4] Southern Research Station, Forest Service, USDA, Pineville, LA, USA

*Corresponding author.
2506 Jacob Drive, Tennessee Forest Products Center, The University of Tennessee, Knoxville, TN 37996, USA
E-mail: swang@utk.edu

Abstract

Refined wood fibers of a 54-year-old loblolly pine (*Pinus taeda* L.) mature wood were investigated by nanoindentation and atomic force microscopy (AFM). The effect of steam pressure, in the range of 2–18 bar, during thermo-mechanical refining was investigated and the nano-mechanical properties and nano- or micro-level damages of the cell wall were evaluated. The results indicate that refining pressure has important effects on the physical and mechanical properties of refined fibers. No obvious damage was observed in the cell walls at pressures between 2 and 4 bar. Nano-cracks (most less than 500 nm in width) were found in fibers at pressures in the range of 6–12 bar, and micro-cracks (more than 5 μm in width) were found in fibers subjected to pressures of 14 and 18 bar. The damages caused at higher pressures were more severe in layers close to the lumen than on the fiber surfaces. Under special circumstances, the S_3 layer was heavily damaged. The natural shape of the cross sectional dimensions of the cell walls was not changed at lower pressures (2 and 4 bar), but, as pressure was increased, the fibers tended to collapse. At pressures around 18 bar, the lumina were augmented again. The nano-mechanical properties in terms of elastic modulus and hardness were obviously decreased, while nanoindentation creep increased with refining pressure.

Keywords: atomic force microscopy (AFM); nanoindentation; nano-mechanical properties; refined fiber; thermo-mechanical refining.

Introduction

In the manufacture of medium-density fiberboard (MDF), thermo-mechanical refining pressure plays an extremely important role in the quality of refined fibers and dominates the performance of final composites. Low refining pressure generates an abundance of fiber bundles as opposed to individual fibers. High pressure may not only shorten the fiber length, but it also damages the fibers otherwise; it induces twisting and curling and lowers the strength of the fibers. Krug and Kehr (2001) suggested that increasing refining steam pressure results in shorter fibers and reduced strength of fiberboard. Kelley et al. (2005) found that with increasing refining pressure, the amount of extractives and glucose was increased while the percentages of xylose, galactose, and mannose decreased.

Fiber strength and morphology (Jones 1960; McMillan 1969), fiber size distribution and bulk density (Myers 1983; Groom et al. 1999) and pH and buffering capacity (Park et al. 2001; Xing et al. 2006) are all important to the properties of the final fiberboard composites. The mechanical properties of individual fibers are most significant with this regard. Jones (1960) demonstrated this for MDF and for high-density fiberboard (HDF) composites. The interrelation between fiber strength, such as stiffness, hardness and creep behavior, and fiberboard properties are still not very clear.

In wood plastic composites (WPCs), wood fibers are supposed to be the reinforcing element. In current WPCs, wood is applied as flour (obtained by grinding sawdust and industrial wood waste) that requires high-energy consumption. The reinforcement potential of wood flour is limited due to the small particle aspect ratio, which does not allow efficient stress transfer from the matrix to the particulates. Clearly, alternative (energy saving and economic) approaches for size reduction of solid wood are needed. The steam explosion is such an alternative (Yin et al. 2007). An optimized refining process could be another alternative.

Kersavage (1973) and Mott et al. (1995) developed methods to measure the tensile modulus of a single wood pulp fiber based on environmental scanning electron microscope (ESEM) and video image analysis (VIA). The tensile test characterizes only the weakest zone of the fiber. Thermo-mechanically refined wood does not contain individual fibers as pulp but fiber bundles instead. These have a more complicated morphology, and the application of the ESEM-VIA method is difficult.

The nanoindentation technique is a new tool for testing the micro- or nano-mechanical properties of near-surface layers of solids. It has been used to measure the longitudinal hardness and modulus of elasticity (MOE) of individual wood cell walls (Wimmer et al. 1997; Gindl et al. 2004; Wang et al. 2006; Tze et al. 2007), the regenerated cellulose fibers (Gindl et al. 2006; Lee et al. 2007a) and the interphase mechanical properties between cellulose

fibers and thermoplastic polymers (Lee and Wang 2005; Lee et al. 2007b).

However, the effect of refining pressure on the cell wall properties of refined wood fibers is still not well understood. Therefore, the objective of this study was to close this gap. The effects of pressure during thermo-mechanical refining should be investigated in terms of the physical and nano-mechanical properties of wood fiber cell walls by means of nanoindentation and AFM.

Materials and methods

Materials and preparation of specimen

A 54-year-old loblolly pine (*Pinus taeda* L.) was collected from a traditional plantation located in Crossett, AR, USA. Mature wood was cut from growth rings representing years 25 to 54 by means of a portable sawmill with ripsaws. Chips were produced at the Southern Research Station (SRS) in Pineville, LA, USA and the chips were refined at pressures of 2, 4, 6, 8, 10, 12, 14 and 18 bar with a thermo-mechanical refiner to generate fibers in the BioComposites Center pilot plant, Bangor, Gwynedd, UK. The fibers were air dried at 23°C and 65% relative humidity (RH) for 2 weeks and embedded in epoxy resin with a silicon mold. The embedded samples were placed in a desiccator under vacuum for 20 min to remove the air bubbles and then cured in an oven at 70°C for 8 h.

The cured sample was cut into a small block and glued to an acrylic block, and the top surface was trimmed with new razor blades to form a small trapezoidal base. The acrylic block was then mounted onto an ultramicrotome, and the top face was cross-sectioned with a glass knife. Finally, the top surface was smoothed with a diamond knife. The final specimens were conditioned at 21°C and 65% RH for at least 24 h in the test room before the nanoindentation test.

Nanoindentation

All indentations were made by a Nano Indenter II (MTS Systems Corp.) equipped with a diamond Berkovich tip (a three-sided pyramidal tip) at the Oak Ridge National Laboratory (Oak Ridge, TN, USA). The indentation experiment consisted of four segments. A rate of 10 nm s^{-1} and 9000 nm approaching distance were used for the first segment. Once the tip contacted the sample surface, a constant strain rate of 0.05 s^{-1} was applied until a designed indentation depth of 200 nm was reached (Figure 1). At this depth, the maximum loading force was held for 10 s prior to the ultimate unloading. This holding segment is not essential, but it offers an opportunity to monitor possible creep or mechanical stabilization of the test materials (Fischer-Cripps 2002).

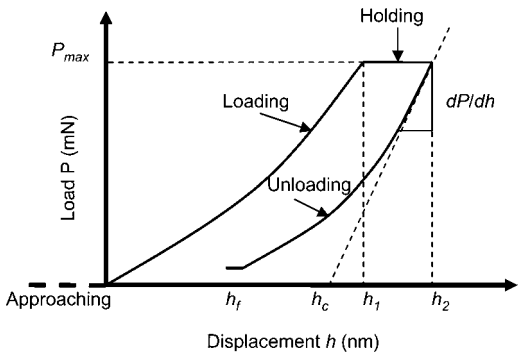

Figure 1 Typical load-displacement curve with the definition of h_f, h_c, h_1 and h_2.

In the unloading segment, a constant displacement rate of 10 nm s^{-1} was applied until 90% of the maximum loading force was removed. At the end of the experiment, the sample was examined by the video system of the Nano Indenter II to evaluate the position and quality of indents. A total of 40 indents were made on 5–9 refined fibers for each sample.

Based on the theory of nanoindentation, the reduced modulus, E_r (the composite modulus for indenter and sample combination) can be evaluated from the nanoindentation measurements by employing the following equation (Oliver and Pharr 1992):

$$E_r = \frac{\sqrt{\pi}(dP/dh)_{unloading}}{2\sqrt{A_{hc}}} \quad (1)$$

where, P is the indentation load; h and h_c are the penetration and contact depths, respectively, and A_{hc} is the contact area, which is a function of the contact depth.

The contact depth at the maximum load is given by:

$$h_c = h_{max} - 0.75\frac{P_{max}}{S} \quad (2)$$

where, $S = dP/dh$ at $h = h_{max}$, and 0.75 is a constant that depends on the indenter geometry. For evaluating E_r, the contact stiffness, $(dP/dh)_{unloading}$, and the contact area A_{hc} could be determined accurately from load against displacement graph measured during the indentation process.

The expression for the contact area using the Berkovich indenter is approximated by the following formula:

$$A = 24.5h_c^2 \quad (3)$$

The hardness (H) can be obtained from the following equation:

$$H = \frac{P_{max}}{A} \quad (4)$$

The sample modulus (E_s) can be calculated as follows:

$$E_s = (1-\nu_s^2)\left(\frac{1}{E_r} - \frac{1-\nu_i^2}{E_i}\right) \quad (5)$$

where, E_s is Young's modulus and ν_s is Poisson's ratio of the specimen; E_i and ν_i are the corresponding values of the indenter. For the diamond indenter used in our experiments, $E_i = 1141$ GPa and $\nu_i = 0.07$. Also, in all calculations, ν_s is assumed to be 0.25. From Eqs. (1)–(6), Young's modulus and the hardness of the fiber cell wall can be obtained.

Indentation creep ratio C_i was defined as the relative change in indentation depth while the applied load remained constant during the holding time (CSM Instruments 2002):

$$C_i = \frac{h_2 - h_1}{h_1} \times 100, \quad (6)$$

where h_2 is the final penetration depth at the end of holding segment, h_1 is the depth at the end of loading segment.

Atomic force microscopy (AFM) and polarized light microscopy

The topographies of the samples were determined by AFM XE-100 (PSIA Corp., Sang-Daewon-Dong, Korea) operated in

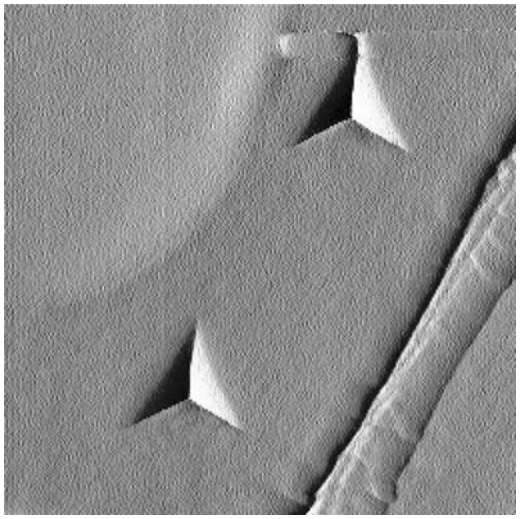

Figure 2 An AFM image of nanoindentation indents in refined fiber cell wall.

contact mode. The surface of the specimens had a vertical range of 300–350 nm with root mean square surface roughness amplitude of 30–35 nm and an average roughness of 20–30 nm. Figure 2 shows the AFM image of indents in the cross sections of the fibers. The damages to the cell walls of the fibers were analyzed by means of the XEI software associated with the AFM. The polarized light microscope (PLM Olympus BX 51, Tokyo, Japan) and its associated software (ImageJ, Bethesda/MD, USA) were also used to obtain and analyze images of the refined fibers.

Results and discussion

Indent position

In general, the S_2 layer comprises approximately 80% of the thickness of the cell walls. Thus, the properties of the S_2 layer are essential for the mechanical properties of the fibers. Accordingly, most indentation tests were performed on the S_2 layers with a few exceptions. For a reliable data analysis, results taken from outside the S_2 layer has to be eliminated. Based on microscope images, indentations taken from overlapped areas or which were outside the edge of the cell wall can be clearly observed. On the other hand, it is very difficult to recognize the indentations taken from defected areas, which are just below the surface (such as micro-cracks), and those from the interface between S_2 and S_1 or between S_2 and S_3 layers, as well as at the interface of the embedded resin and S_1 or S_3.

The locations of all indentations taken from the material obtained at lower steam pressures can be classified into five zones. The combination of microscopy and the load/displacement curve of each indentation are helpful with this regard (Figure 3a). The same is true for the six classification zones for fibers refined at higher steam pressures (14–18 bar) (Figure 3b). The first zone is for the overlapped indentations. These have the highest P_{max}. This could be due to the plastic deformation by the first indentation, which makes the cell wall denser. When a second indent should add on this denser cell wall area,

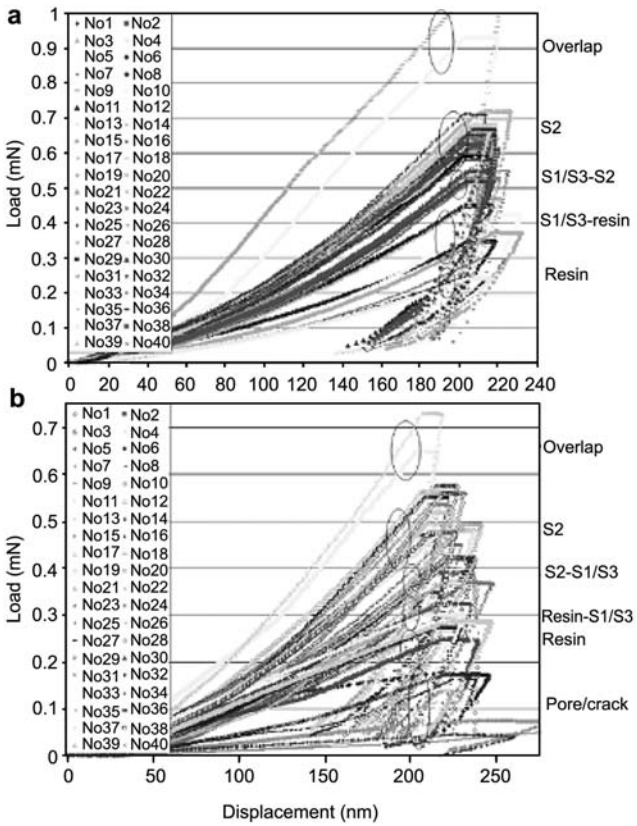

Figure 3 Load-displacement curves of indents. (a) Refined fibers obtained at 2 bar, (b) refined fibers obtained at 18 bar.

higher force would be needed to penetrate the same depth. The second zone is for the indentations in the S_2 layer without defects. The third zone is the interphase of S_2 and S_1 or that of S_2 and S_3. The fourth zone is the interface between the embedded resin and the cell wall. The fifth zone is the embedded resin. The last zone is for indentations taken on large defects, such as micro-pores or cracks in the cell walls of the fibers. However, the indents in S_2 layers with small cracks can be in the zones of 2–5.

The effects of refining pressure on damage and morphologies of fiber cell walls

No obvious damage was observed in the cross section of fibers treated at lower pressures (2 and 4 bar). As pressure increased, however, nano-cracks were found in the cell wall, especially on the thinner part of the cell wall (Figure 4a). The width of most crackles was less than 500 nm, as measured with AFM. Micro-cracks were observed in the cell wall cross section of fibers at higher pressures (14 and 18 bar). Some cracks were more than 5 μm in width. It seemed that the micro damages in layers close to the lumen were more serious than those close to the compound middle lamella (Figure 4b). The S_3 layer in Figure 4b was heavily damaged, but in Figure 4a, the S_3 layer is not obviously affected. The sudden explosion of the higher pressures inside the lumens, as the fibers are released from the refiner, is the reason for damages on the S_3 layer. Yin et al. (2007) also found that the rupture of chips was more likely to occur by exploding cells from their lumens than by separating cells along their middle lamellae.

The cross sectional dimensions of the cell walls at pressures of 2 and 4 bar remained almost unchanged. This could be due to the fact that more than 68% of the fibers were present as fiber bundles, as shown in Figures 5 and 6. As refining pressure increased to 6 bar, the amount of fiber in bundles was greatly diminished to 30% and to 7% at 18 bar treatment. The lumen of fibers tended to collapse, as clearly visible on their narrow cross section. Cross-sectional stability of the fibers can be described by their ratio of length (L) to width (W), i.e., L/W, as listed in Table 1. L/W increased from 1.4 to 2.5 as refining pressure increased from 2 bar to 12 bar.

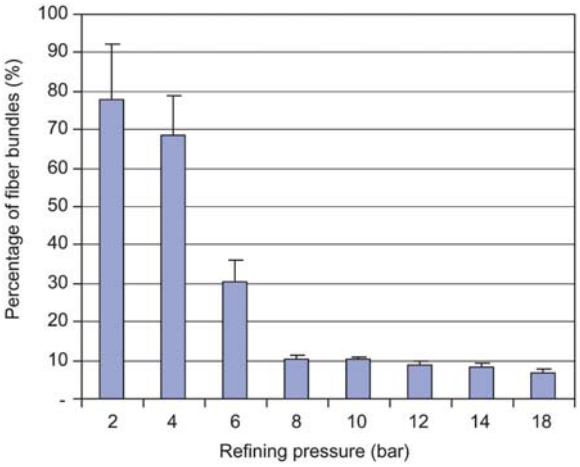

Figure 5 Percentage of fiber bundles as a function of refining pressure.

This could be explained by the hypothesis that the swollen fibers collapse more readily between the refiner plates under higher steam pressure conditions. Another or additional explanation could be that the wet fibers tend to collapse as different shrinkages occur in different directions during the fiber drying process. In addition, as curling and twisting increased, the extent of collapse also increased. However, when pressure was elevated to 18 bar, the size of the cross sections obviously decreased and the L/W ratio decreased to 1.83. As wood fibers are refined at higher pressure, some substances of the cell walls can be degraded (hydrolyzed). This can lead to a shrinkage of fiber diameter after drying. The change of the lumen from a narrow to a round shape is probably due to the gas extension after the pressure is released. This could be the reason why the L/W decreased in fibers produced at 14 and 18 bar.

The effect of refining pressure on the mechanical properties of the fiber cell walls

The nanoindentation results of fiber cell wall mechanical properties are summarized in Table 2. The fibers at the lowest pressure (2 bar) exhibited the highest elastic modulus (21 GPa). This value is higher than that of the natural

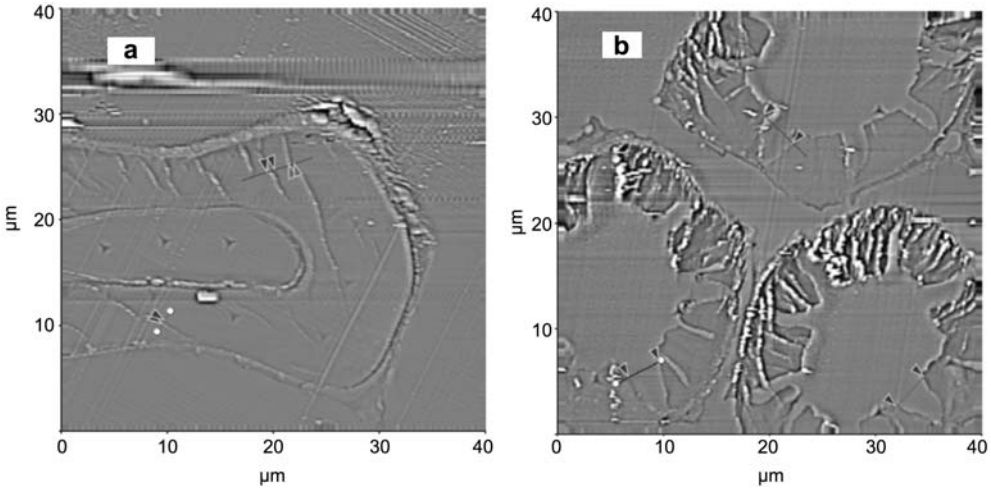

Figure 4 Damages in refined fiber cell wall cross sections. (a) Refined fibers obtained at 8 bar, (b) refined fibers obtained at 18 bar.

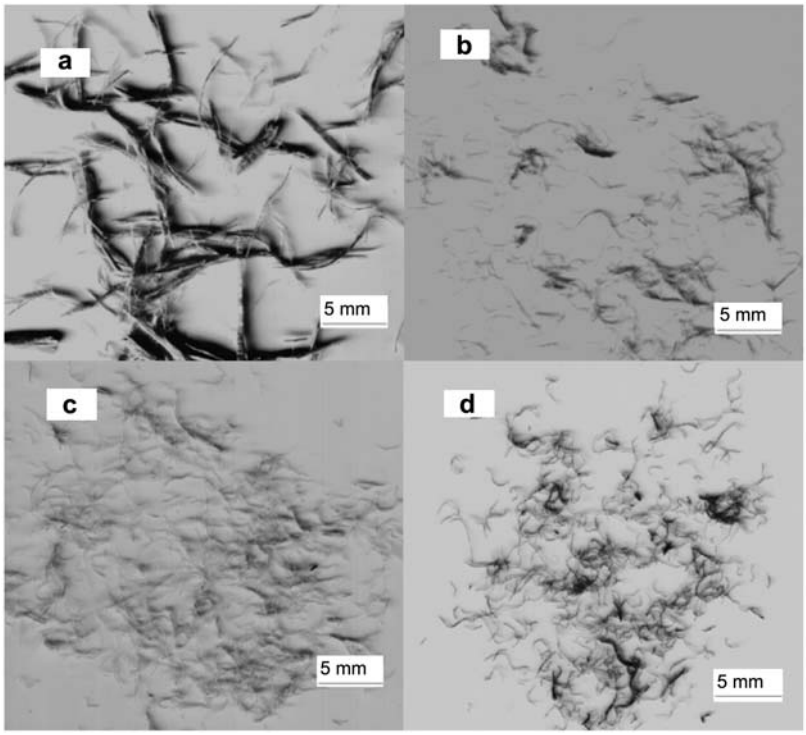

Figure 6 Refined fibers from different pressure: (a) 4 bar, (b) 6 bar, (c) 8 bar, (d) 14 bar.

Table 1 Fiber cell wall cross sectional dimensions with refining pressures.

	Steam pressure (bar)							
	2	4	6	8	10	12	14	18
L (μm)	35.4 (2.18)	33.6 (1.29)	37.3 (3.71)	40.5 (6.21)	41.5 (5.67)	41.1 (3.16)	37.1 (6.23)	28.3 (4.79)
W (μm)	24.8 (2.66)	23.4 (1.65)	22.4 (4.41)	22.4 (3.66)	21.1 (6.75)	16.6 (2.14)	21.5 (1.06)	15.5 (3.89)
L/W	1.43 (0.14)	1.44 (0.13)	1.66 (0.23)	1.81 (0.36)	1.97 (0.66)	2.48 (0.29)	1.73 (0.33)	1.83 (0.67)

L, Length; W, width. L/W, Ratio of length and width. Data in parentheses are standard deviations.

Table 2 Summary of nanoindentation results of fiber cell wall.

Property[a]		Steam pressure (bar)							
		2	4	6	8	10	12	14	18
	Mean	21.35	18.62	15.96	16.83	15.32	14.05	13.09	12.22
Es	SD	2.59	2.97	2.41	2.53	2.51	2.87	3.42	3.29
GPa	CV	12.13	15.95	15.10	15.03	16.38	20.43	26.13	26.92
	Mean	0.50	0.47	0.47	0.45	0.43	0.43	0.39	0.37
H	SD	0.04	0.062	0.07	0.05	0.067	0.079	0.078	0.095
GPa	CV	8.00	13.19	14.89	11.11	15.58	18.37	20.00	25.68
	Mean	7.58	8.72	8.87	8.63	8.24	9.68	12.30	13.08
Ci	SD	0.86	1.56	1.25	1.29	1.09	1.79	3.89	3.91
%	CV	11.35	17.89	14.09	14.95	13.23	18.49	29.25	29.89
n		31	27	23	28	30	28	14	13

[a]SD, standard deviation; CV, coefficients of variation; Ci, indentation creeps; n, the number of indents. Es, elastic modulus; H, hardness.

(unpressurized) cell wall of the same wood (Tze et al., 2007). This indicates that lower pressure has a reinforcement effect on the mechanical properties of fiber cell walls. However, this effect only appeared on fibers subjected to a pressure of 2 bar.

Runkel and Wilke (1951) reported that hemicelluloses in beech and spruce, which are the least thermal stable component compared to lignin and cellulose, decreased at temperatures between 130°C and 194°C. Also for the mild conditions in this study (2 bar, 134°C) it can be assumed that no fiber degradation occurs. The structural alteration in the cell wall during refining and drying may lead to the reinforcement of the cell walls. The results of Yildiz et al. (2002) and Repellin and Guyonnet (2003) also support the finding that MOE of wood can be improved by thermal treatment.

On the other hand, fibers subjected to pressures between 4 and 18 bar (at 152–210°C) can cause some degradation in the cell wall. This leads to stiffness decrement of fibers. The elastic moduli (EM) of fibers in the

present study (treatment at 4–10 bar) were similar (18.6–14.1 GPa) to those obtained from natural wood fibers described by Tze et al. (2007). These EM data of the highest pressure fibers were 9 GPa lower than those obtained from fibers treated at milder conditions (2 bar). It is obvious that refining pressure has a significant effect on the mechanical properties of fibers, because at harsh conditions the cell wall is damaged.

Wet and swollen fibers also suffered chemical changes under harsh conditions. Fibers subjected to 18 bar (210°C) refining conditions could result in the degradation of hemicelluloses, lignin and cellulose. The macroscopic observations of the fiber furnish with dark appearance reveals numerous fine cracks. The reduction of the MOE in fiber walls is plausible based on these observations.

The EM observed in this study were 2–3 times greater than the tensile moduli (from 2.7 to 8.5 GPa) reported by Groom et al. (2006) for fibers of the same origin. Tensile tests are indicative of the entire cross section of the fibers, including the primary cell wall, the secondary cell wall and the middle lamella. The EM of the S_2 layer are significantly greater than those of other layers. According to Lee et al. (2007a), there is no significant difference in moduli of Lyocell fibers deduced by nanoindentation and the nano-tensile test. However, the homogeneity of Lyocell fibers is high; they have a regular morphology and are defect-free. Accordingly, the performance of the tensile tests was more accurate. On the other hand, the nanoindentation has the advantage that the effects of the largest fiber damage do not play an essential role. The same is true for the irregular fiber morphology. Accordingly, the nanoindentation emphasizes the mechanical properties of the cell wall (i.e., S_2 layer) as affected by refining steam pressure.

The hardness was influenced by refining conditions in a similar way, but the differences were smaller than those of elasticity moduli. The hardness values decreased from 0.50 to 0.43 GPa as refining pressure increased from 2 to 12 bar. At pressures between 14 and 18 bar, hardness values were further reduced to 0.39 and 0.37 GPa. The higher the refining pressure, the more cracks are formed in the cell wall. Obviously, the cell wall density – as a main contributor to the hardness – decreases in the presence of cracks in the cell wall. The indentation creep increment varied from 7.6% to 9.7% for fibers subjected to pressures of 2–12 bar, but increased to 12.3% for a pressure of 14 bar and to 13.1% for a pressure of 18 bar. Cell wall damages of fibers subjected to pressures over 14 bar are indeed serious.

Conclusion

The physical and mechanical properties of refined wood fiber cross section can be successfully investigated by nanoindentation and AFM techniques. The exact location and penetration pattern of each indentation can be accurately determined from the load/displacement curves associated with indentation images. Refining pressure was a very important determinant of the physical and mechanical properties of refined fibers. No obvious damage was observed in the fiber cross section for fibers subjected to lower pressures (2 and 4 bar). Nano-cracks were found in fibers subjected to pressures of 6–12 bar, and micro-cracks were found in fibers subjected to higher pressure (14 and 18 bar). The cross sectional dimension was more stable for fibers subjected to lower pressures than for fibers subjected to higher pressures. The nano-mechanical properties of refined fibers decreased with pressure. The nanoindentation creep was higher after application of higher pressures than at lower pressures.

Acknowledgements

The authors wish to thank Drs. John Dulap and Seung-Hwan Lee for their kind help for preparing the samples. The project was supported by the National Research Initiative of the USDA Cooperative State Research, Education and Extension Service, grant number # 2005-02645 and the USDA Wood Utilization Research Grant. Instrumentation for the nanoindentation work was provided through the SHaRE Program at the Oak Ridge National Laboratory, which was sponsored by the Division of Materials Science and Engineering, U.S. Department of Energy, under contract DE-AC05-000R22725 with UT-Battelle, LLC.

References

CSM Instruments (2002) Overview of mechanical test standards. Applications bulletin No. 18.

Fischer-Cripps, C.A. Nanoindentation. Springer-Verlag, New York Inc., 2002. 197 pp.

Gindl, W., Gupta, H.S., Schöberl, T., Lichtenegger, H.C., Fratzl, P. (2004) Mechanical properties of spruce wood cell walls by nanoindentation. Appl. Phys. A 79:2069–2073.

Gindl, W., Konnerth, J., Schöberl, T. (2006) Nanoindentation of regenerated cellulose fibers. Cellulose 13:1–7.

Groom, L.H., Mott, L., Shaler, S.M. (1999) Relationship between fiber furnish properties and the structural performance of MDF. In: Proceedings of the 33rd International Particleboard/ Composite Materials, Pullman, WA, USA. P89–100.

Groom, L.H., So, C.L., Elder, T., Pesacreta, T., Rials, T.G. (2006) Effects of refiner pressure on the properties of individual wood fibers. In: Characterization of the Cellulosic Cell Wall. Eds. Stokke, D., Groom, L. Blackwell Publishing, Ames, Iowa, USA. Chapter 17, pp. 227–240.

Jones, E.J. (1960) The relation of fiber and pulp properties to the properties of structural fiberboard products. Tappi 43: 600–602.

Kelley, S.S., Elder, T., Groom, L.H. (2005) Changes in the chemical composition and spectroscopy of loblolly pine medium density fiberboard furnish as a function of age and refining pressure. Wood Fiber Sci. 37:14–22.

Kersavage, P.C. (1973) A system for automatically recording the load-elongation characteristics of single wood fibers under controlled relative humidity conditions. USDA, US Government Printing Office, Washington, DC, USA. 46 pp.

Krug, D., Kehr, E. (2001) Influence of high pulping pressures on permanent swelling-tempered medium density fiberboard. Holz Roh Werkst. 59:342–343.

Lee, S.H., Wang, S. (2005) Characterization of interfacial properties between cellulose fiber and thermoplastic by AFM and nanoindentation. In: The 230th ACS National Meeting, Division of Industrial and Engineering Chemistry, Washington, DC, Aug 28–Sept 1, 2005, Abstract.

Lee, S.H., Wang, S., Pharr, G.M., Kant, M., Penumadu, D. (2007a) Mechanical properties and creep behavior of lyocell fiber using nanoindentation and nano-tensile testing. Holzforschung 61:254–260.

Lee, S.H., Wang, S., Pharr, G.M., Xu, H. (2007b) Evaluation of interphase property in a cellulose fiber-reinforced polypropylene composite by nanoindentation and finite element

analysis. Composites Part A: Appl. Sci. Manufact. 38: 1517–1524.
McMillan, C.W. (1969) Fiberboards from loblolly pine refiner groundwood: aspects of fiber morphology. Forest Prod. J. 19:56–61.
Mott, L., Shaler, S., Groom, L.H., Liang, B. (1995) The tensile testing of individual wood fibers using environmental scanning electron microscopy and video image analysis. Tappi 78:143–148.
Myers, G.C. (1983) Relationship of fiber preparation and characteristics to performance of medium-density hardboards. Forest Prod. J. 33:43–51.
Oliver, W.C., Pharr, G.M. (1992) An improved technique for determining hardness and elastic modulus using load and displacement sensing indentation experiments. J. Mater. Res. 7: 1564–1583.
Park, B.D., Kim, Y.S., Riedl, B. (2001) Effect of wood-fiber characteristics on medium density fiberboard (MDF) performance. J. Korean Wood Sci. Technol. 29:27–35.
Repellin, V., Guyonnet, R. (2003) Evaluation of heat treated beech by unrestrictive testing. In: The First European Conference on Wood Modification, Ghent, Belgium, April 2003. P73–82.
Runkel, R.O.H., Wilke, K.D. (1951) Chemical composition and properties of wood heated at 140 to 200C in a closed system without free space. Part II. Holz Roh Werkst. 9:260–270.
Tze, W.T.Y., Wang, S., Rials, T.G., Pharr, G.M., Kelley, S.S. (2007) Nanoindentation of wood cell walls: continuous stiffness and hardness measurements. Composites: Part A: Applied Science and manufacturing, 38:945–953.
Wang, S., Lee, S.H., Tze, W.T.Y., Rials, T., Pharr, G.M. (2006) Nanoindentation as a tool for understanding nano-mechanical properties of cell wall and biocomposites. In: International Conference on Nanotechnology for the Forest Products Industry, Marriott Marquis, Atlanta, GA, April 26–28. 7 pp.
Wimmer, R., Lucas, B.N., Tsui, T.Y., Oliver, W.C. (1997) Longitudinal hardness and Young's modulus of spruce tracheid secondary walls using nanoindentation technique. Wood Sci. Technol. 31:131–141.
Xing, C., Zhang, S.Y., Deng, J., Riedl, B., Cloutier, A. (2006) Medium-density fiberboard performance as affected by wood fiber acidity, bulk density, and size distribution. Wood Sci. Technol. 40:637–646.
Yildiz, S., Colakoglu, G., Yildiz, U., Gezer, E., Temiz, A. (2002) Effects of heat treatment on modulus of elasticity of beech wood. The International Research Group on Wood Preservation; IRG Document No. IRG/WP 02-40222.
Yin, S., Wang, S., Rials, T.G., Kit, K., Hansen, M. (2007) Polypropylene composites filled with steam-exploded wood flour from insect-killed loblolly pine by compression-molding. Wood Fiber Sci. 39:95–108.

Received July 23, 2007. Accepted November 28, 2007.